EVs Containing Host Restriction Factor IFITM3 Inhibited ZIKV Infection of Fetuses in Pregnant Mice through Trans-placenta Delivery

Xue Zou,[1] Meng Yuan,[1] Tongyu Zhang,[4] Nan Zheng,[1,2,3] and Zhiwei Wu[1,2,3]

[1]Center for Public Health Research, Medical School, Nanjing University, Nanjing, China; [2]State Key Laboratory of Analytical Chemistry for Life Science, Nanjing University, Nanjing, China; [3]Medical School, Jiangsu Key Laboratory of Molecular Medicine, Nanjing University, Nanjing, China; [4]Model Animal Research Center, Nanjing University, Nanjing, China

Zika virus (ZIKV) infection can lead to neurological complications and fetal defects, and it has attracted global public health concerns. Effective treatment for ZIKV infection remains elusive, and a preventative vaccine is not yet available. Therapeutics for fetuses need to overcome placenta barriers to reach the fetuses and require higher safety standards. In the present study, we engineered mammalian extracellular vesicles (EVs) to deliver a host restriction factor, interferon-induced transmembrane protein 3 (IFITM3), for the treatment of ZIKV infection. Our results demonstrated that the IFITM3-containing EVs (IFITM3-Exos) suppressed ZIKV viremia by a 2-log reduction in pregnant mice. Moreover, the engineered EVs effectively delivered IFITM3 protein across the placental barrier and suppressed ZIKV in the fetuses with significant reduction of viremia in key fetal organs as measured by quantitative real-time PCR. Mechanistic study showed that IFITM3 was delivered to late endosomes/lysosomes where it inhibited viral entry into the host cells. Our study demonstrated that EVs could act as a cross-placenta drug delivery vehicle to the fetus, and IFITM3, an endogenous restriction factor, is a potential treatment for ZIKV infection during pregnancy.

INTRODUCTION

Zika virus (ZIKV), a member of Flaviviridae, infects humans mostly through bites of *Aedes* mosquito species. Usually, ZIKV infection only causes mild symptoms such as rash, conjunctivitis, and short-term fever. However, it can also cause a birth defect called microcephaly and other severe brain defects in the developing fetus and in newborns. During the past two decades, there were at least three ZIKV outbreaks in the world. The latest outbreak in 2015 was first reported in Brazil and then spread to 86 countries, resulting in 4,783 suspected associated microcephaly cases in Brazil alone.[1] Antiviral treatment is needed particularly for severely infected patients with prolonged viremia or for individuals during pregnancy.[2,3] However, there has been no specific treatment available for ZIKV infection or its complications until now.[4] Considering that the fetus is susceptible to side effects of therapeutics, it is a challenge to develop safe chemotherapy to treat ZIKV infection during pregnancy. As ZIKV is detected in placenta and fetal tissues, anti-viral therapeutics need to be delivered across the placental barrier to the fetus, and the safety of the therapeutics needs to meet the high standards for a developing fetus.

Interferon (IFN)-induced transmembrane protein 3 (IFITM3) is an intrinsic cellular factor that restricts infections by several important viral pathogens.[5,6] IFITM3 is mainly located on the endolysosomal membrane, playing a suppressor role at an early stage of viral replication.[7] It can inhibit the entry of viruses by preventing virus fusion with endolysosomal membranes, thus limiting the infection.[8] Notably, IFITM3 has been shown to potently inhibit ZIKV infection.[9,10] IFITM3 is also highly expressed in the placenta, and its expression is elevated during pregnancy,[11] suggesting that IFITM3 plays roles in fetus defense against pathogens[12] and it is likely well tolerated by and safe for the developing fetus.

Extracellular vesicles (EVs), especially exosomes, defined as cell-originated vesicles with phospholipid membrane ranging from 40 to 150 nm in diameter and derived from endocytic compartment,[13] secreted by a variety of live cells, and transporting bioactive molecules between cells, play important roles in cell-cell interactions. Exosomes contribute to immune regulation, tumor metastasis, and other physiological processes.[14] Moreover, using exosomes as a nano-delivery vehicle to deliver functional RNAs or small molecules into target cells and tissues for the treatment of diseases, including infectious diseases and tumors,[15–17] is a hot research topic. However, studies on the delivery of protein by exosomal vehicles have remained insufficient. IFITM3 is a transmembrane protein and exerts its antiviral effects only when it is correctly positioned on the membrane of lysosomes or late endosomes. Its transmembrane structure poses a challenge for cross-cell delivery. A recent study reported that during dengue

---
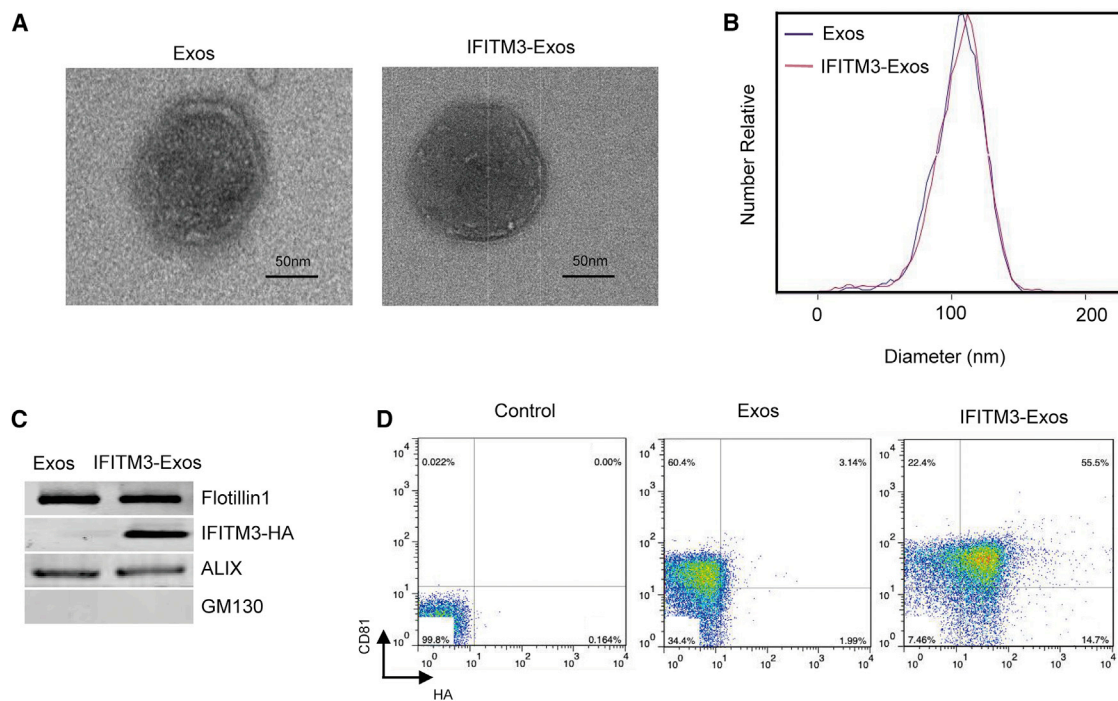
Figure 1. Analysis of IFITM3-Exos Derived from 293T Cells

(A) TEM images of Exos and IFITM3-Exos. Scale bars, 50 nm. (B) Size distributions of Exos and IFITM3-Exos were measured by NTA. The median diameters were 118.9 nm for Exos and 126 nm for IFITM3-Exos. (C) Western blots of exosomes prepared from supernatants of 293T cell culture. IFITM3-Exos were prepared from the cells that had been transfected with pHA-IFITM3 encoding IFITM3 and HA-tag. The quality of each exosome preparation was confirmed by the presence of exosomal marker ALIX and Flotillin 1, and the absence of Golgi marker GM130. (D) CD81, the surface marker of EVs, as well as HA-tag of IFITM3 were detected by flow cytometry for both Exos and IFITM3-Exos. Exos prepared from 293T cells were absorbed on latex beads and then subjected to antibody staining.

virus infection, exosomes could deliver IFITM3 intercellularly and thus transmit its antiviral effect from the virus-infected cells to the un-infected cells,[18] making it possible to use exosomes as a delivery vehicle for IFITM3 to treat viral infection.

Furthermore, some evidence indicated that exosomes could pass through the placental barrier and transport signals between the mother and the fetus,[19] providing a possibility of using exosomes as a delivery vehicle for therapeutics into the fetus. Maternal exosomes reaching the fetal tissues could play functional roles in the recipients, resulting in fundamental biological consequences.[20,21] In the present study, we engineered IFITM3-containing EVs (IFITM3-Exos), delivered the IFITM3-Exos across the placenta via the tail veins of pregnant mice, and investigated the inhibition of ZIKV replication in the mice and the fetuses for the development of a specific treatment of ZIKV infection. It is also important to determine feto-maternal exosome trafficking and function during pregnancy. We showed that IFITM3-Exos delivered IFITM3 molecules and specifically suppressed ZIKV infection both in the mothers and in their fetuses, by using cell culture and pregnant mouse models. Our study demonstrated that exogenous IFITM3 delivered by an EV vehicle could be a potential therapeutic approach for the control of ZIKV infection during pregnancy.

RESULTS

Preparation of IFITM3-Containing EVs

IFITM3 expression plasmid was transfected into 293T cells to produce IFITM3-Exos. Then, IFITM3-Exos were purified from the culture supernatants of the transfected cells by differential centrifugation, as previously described.[18] The morphology of the purified EVs was examined by transmission electron microscopy (TEM). A typical IFITM3-Exo is shown in Figure 1A. The median particle diameter of the non-engineered EVs (Exos) is 118.9 nm, and that of the IFITM3-Exos is 126.0 nm, as determined by nanoparticle tracking analysis (NTA), as shown in Figure 1B. The expression of IFITM3 on the EVs was examined by the detection of hemagglutinin tag (HA-tag) using an anti-HA antibody and western blot analysis (Figure 1C). In the preparation, the EVs of the particle diameter as exosomes (40–150 nm) were preferentially purified by 110,000 × g ultracentrifugation. Additionally, the presence of exosomal marker ALIX and Flotillin 1, and the absence of Golgi marker GM130, showed that a major part of the purified EVs was exosomes. Furthermore, flow cytometry was performed to measure the surface expression of IFITM3 and the exosomal marker CD81 on the IFITM3-Exos, as shown in Figure 1D. It showed that 55.5% of the CD81-positive EVs expressed IFITM3. EVs derived from 293T cells without IFITM3 transfection (Exos) were purified in the same way and served as a control.
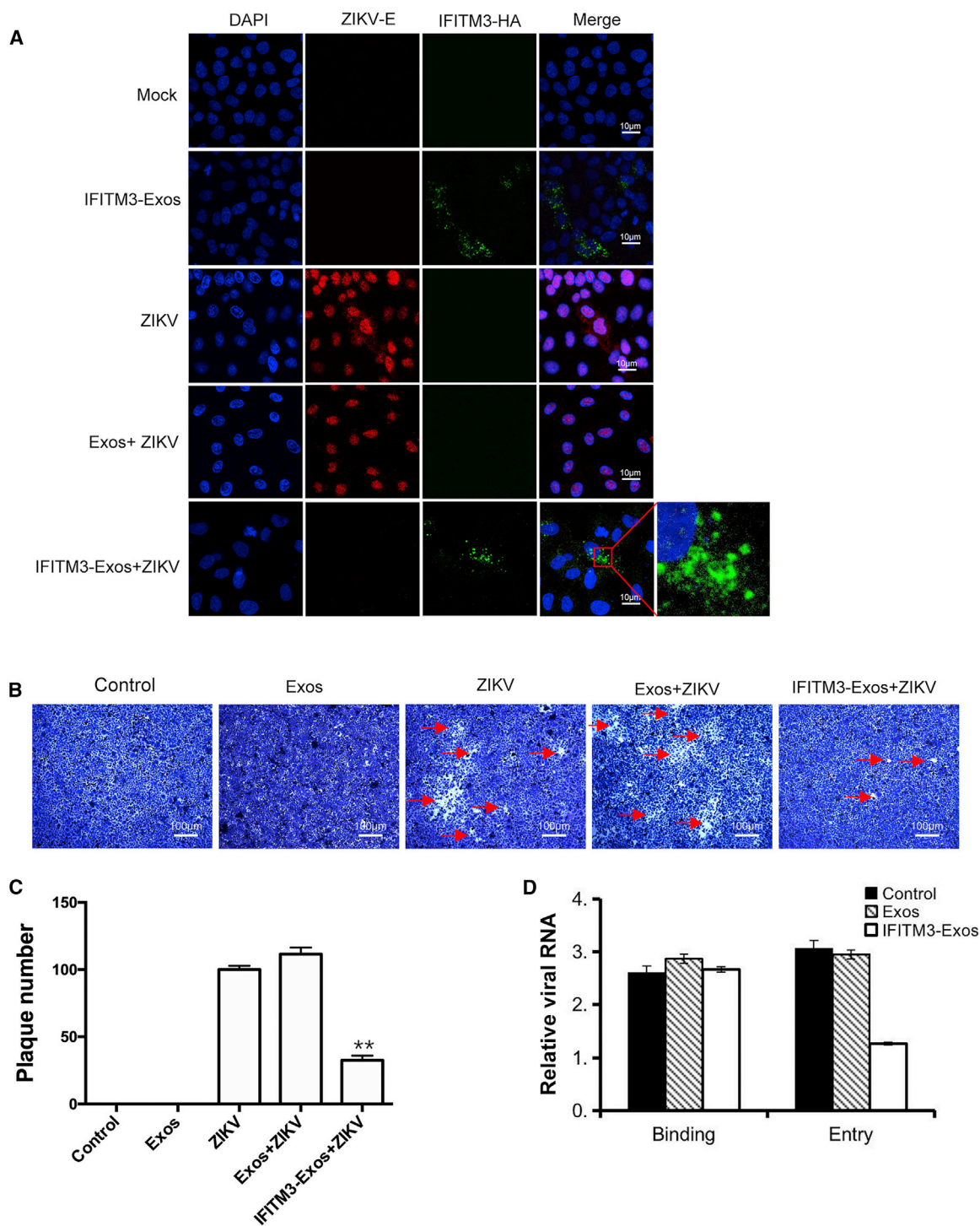
Figure 2. IFITM3-Exos Inhibited ZIKV Infection *In Vitro*

(A) Confocal microscopic images show that IFITM3-Exos (green) inhibited ZIKV infection (ZIKV E protein in red) in Vero cells with DAPI staining of the nuclei (blue). Vero cells were incubated with 60 μg/well of Exos or IFITM3-Exos. For the ZIKV$^+$ samples, the cells were inoculated with ZIKV at 3×10^5 PFU. (B) Plaque assay showed IFITM3-Exos inhibition of viral plaque formation. Vero cells were incubated with 60 μg/well of Exos or IFITM3-Exos. Vero cells were incubated with ZIKV for 2 h (1×10^3 PFU) for virus adsorption and then the viral inoculum was removed and the cells were cultured for 4 days. The cells were then stained with crystal violet for plaque counting. (C) Statistics of the plaque counting(D) Virus binding and entry assays were performed on HeLa cells. HeLa cells were pretreated with IFITM3-Exos or Exos, with the untreated HeLa cells

(legend continued on next page)

IFITM3-Exos Inhibited ZIKV Infection *In Vitro*

To investigate whether IFITM3-Exos would render target cells resistant to ZIKV infection, we treated Vero cells with IFITM3-Exos or EVs without IFITM3 (Exos) followed with ZIKV infection (3×10^5 plaque-forming units [PFU]). To illustrate the suppressor roles of IFITM3-Exos, we simultaneously measured the expression of ZIKV envelope (E) protein and IFITM3 in the ZIKV-infected HeLa cells. The uninfected cells served as negative control (mock). As shown in Figure 2A, IFITM3 was detected in the cytoplasm of IFITM3-Exos-treated cells but not in the mock-treated cells. Compared with the Exos-treated control cells, the IFITM3-Exos-treated cells exhibited strong suppression of ZIKV E protein production. Our results showed that the IFITM3-Exos were delivered to the target cells and that the exogenous IFITM3 inhibited ZIKV infection.

The infection of the cells was further evaluated by a plaque assay at 5 days post-infection. As shown in Figures 2B and 2C, fewer plaques were observed in the cells treated with IFITM3-Exos than in the cells treated with Exos or without treatment. Vero cells treated with IFITM3-Exos exhibited strong resistance to ZIKV (10^3 PFU) infection. To determine whether the IFITM3-Exos-treated cell resistance to ZIKV infection was due to block at the entry, we measured the viral RNA levels in ZIKV-infected cells with or without prior IFITM3-Exos treatment, in both virus binding and entry phases (Figure 2D). At the entry phase the IFITM3-Exos-treated cells exhibited about 1-log reduction of viral RNA as compared with the Exos-treated or untreated cells (Figure 2D). In contrast, in the binding phase, viral RNA showed no differences in cells treated with IFITM3-Exos, Exos, or no treatment. These results indicate that EV-delivered IFITM3 inhibited ZIKV entry into, but not binding to, the host cells.

IFITM3-Exos Specifically Inhibited ZIKV Infection

In order to determine the specific role of IFITM3 in inhibiting ZIKV infection, we investigated the specificity of viral inhibitory activities of IFITM3-Exos and two IFITM3 mutants, IFITM3Δ1–21[22,23] and IFITM3Δ59–68,[24] expressed on EVs in ZIKV infection of Vero cells. IFITM3Δ1–21 loses inhibitory activity against ZIKV entering at endosomes, whereas IFITM3Δ59–68 loses an amphipathic helix related to viral suppression. The IFITM3Δ1–21-Exos and IFITM3Δ59–68-Exos were analyzed by western blot assays of the HA-tag, as well as exosomal marker ALIX and Flotillin 1, which were shown to be successfully expressed on the EVs (Figure S1). Flow cytometric analysis showed that 56.1% and 60.1% of the CD81-positive engineered EVs expressed IFITM3 variants Δ1–21 and Δ59–68, respectively (Figure S3). Upon the delivery of the EVs to the target cells, only the wild-type IFITM3-Exos were located on lysosomes/late endosomes, where the endogenous IFITM3 resides and functions, as shown by the fluorescent signal merge of lysosomal/late endosomal marker Lamp-1 and exosomal label DiI-perchlorate (DiI). Furthermore, we tested the ability of the mutant and wild-type IFITM3-containing exosomes to

inhibit ZIKV replication (Figure 3B). We measured ZIKV E protein expression in the infected Vero cells after EV treatment by flow cytometry (Figure 3B), determined the viability of exosome-treated ZIKV-infected Vero cells (Figure 3C), and showed that only the EVs expressing wild-type IFITM3 suppressed ZIKV replication and protected the cells from virus-induced cytopathic effects; in contrast, the EVs expressing two IFITM3 mutants failed to suppress viral replication or to protect the infected cells. This result is consistent with previous reports that the IFITM3Δ1–21 or IFITM3Δ59–68 loses the biological ability to inhibit viral infection via endosomal pathways.[23,24]

IFITM3-Exos Were Delivered to the Fetuses of Pregnant Mice

ZIKV has been shown to invade placenta and infect fetuses;[25,26] therefore, therapeutics must be delivered across placenta and reach the fetuses to inhibit viral replication. We investigated whether IFITM3-Exos could be delivered in a pregnant mouse to its fetuses by administering DiR iodide (DiR)-labeled IFITM3-Exos to pregnant mice (embryonic day 19.5 [E19.5]) through tail veins at 150 μg of EVs per mouse and then determining the tissue distribution of the EVs. The distribution of IFITM3-Exos in mice was evaluated by an *in vivo* optical imaging system (IVIS) (Xenogen). Figure 4A shows a representative organ distribution of IFITM3-Exos in a pregnant mouse. After 4 h, the EVs spread to all vital organs in the mouse, although most of the DiR-labeled IFITM3-Exos were localized in the liver. Tissue dissection and imaging analysis also showed that the EVs were predominantly detected in the liver of the pregnant mouse (Figure 4B), consistent with a previous study using exosomes for drug delivery.[27] Our results showed that the IFITM3-Exos administered via tail veins could cross the placenta and enter the fetuses in the uterus of the pregnant mouse, as shown in Figures 4C and 4D, suggesting that the EVs entered the fetuses from the maternal circulatory system, making them a potential delivery vector for therapeutics to the fetuses.

IFITM3-Exos Efficiently Penetrated the Placental Barrier

To investigate the efficiency of IFITM3-Exos crossing the placental barrier, we analyzed the penetration of IFITM3-Exos using a placental cell model. BeWo, a human choriocarcinoma cell line representing villous cytotrophoblasts, and H295R, a human adrenocortical carcinoma cell line representing the fetal unit, were cultured in a carefully adapted co-culture system.[28,29] The BeWo cells were planted at the upper chamber of a transwell culture container, and the H295R cells were planted at the lower chamber (Figure 5A). The tight junction formation and the integrity of the BeWo monolayer were monitored by transepithelial electrical resistance (TEER) using a Millicell ESR-2 (Millipore, Bedford, MA, USA).

DiI-labeled IFITM3-Exos were administered into the upper chamber of the transwell culture once the BeWo cells had formed a complete monolayer. After 12 h of incubation, the BeWo cells and the H295R cells were harvested and analyzed by flow cytometry for the

as control. The cells were incubated on ice with ZIKV for 1 h with the presence of IFITM3-Exos or Exos to allow viral binding. For viral entry, the cells were incubated at 37°C for 10 min after the 1-h incubation on ice. qRT-PCR was performed to determine the quantity of viral genomes that had entered cells, and relative viral RNA was shown. Data are mean ± SEM from triplicate assays. *p < 0.05, **p < 0.01.
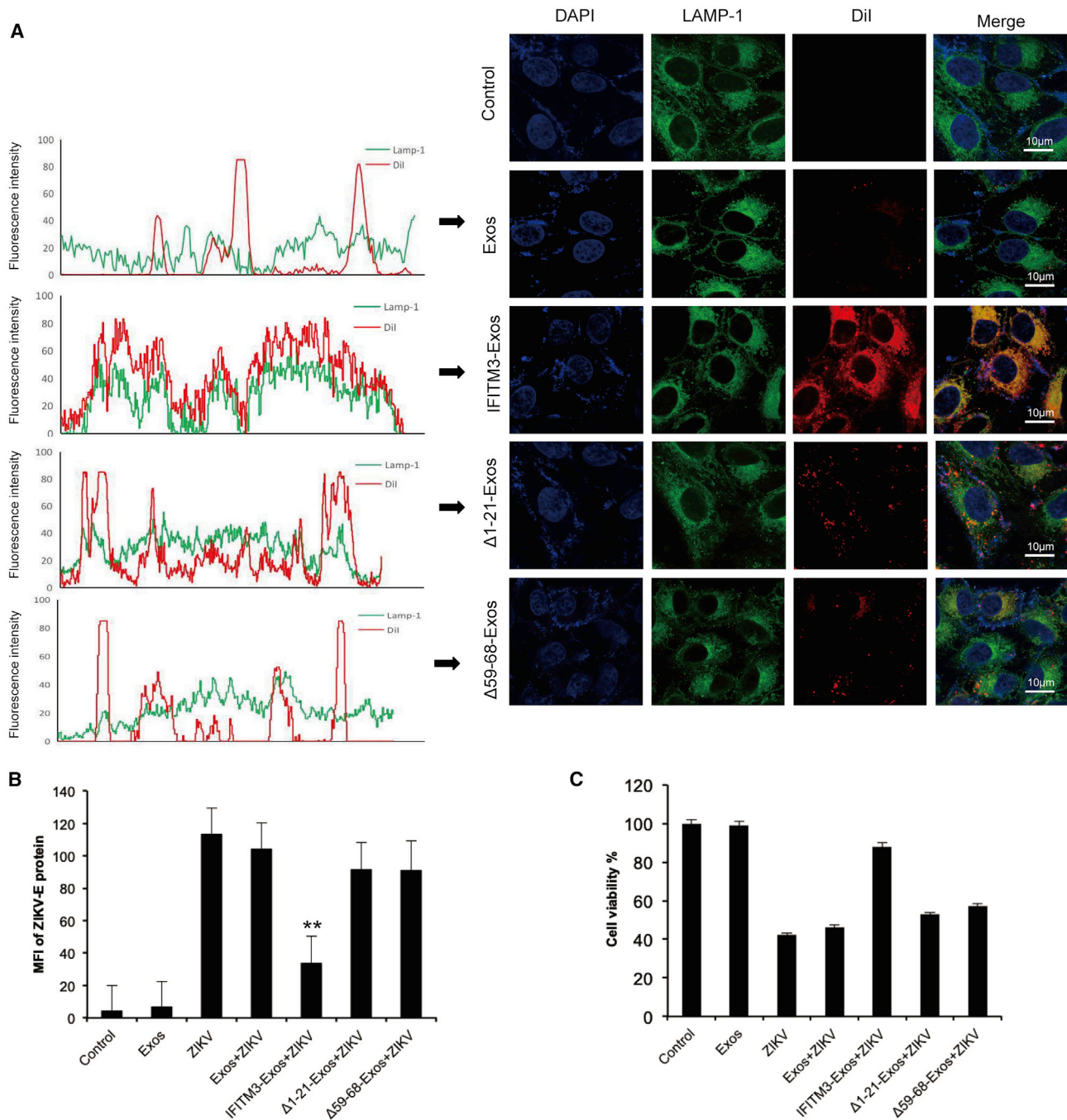
Figure 3. Exosomes Carrying Mutant IFITM3 Δ1–21 or Δ59–68 Failed to Localize to Endolysosomes and Could Not Inhibit ZIKV

(A) Confocal microscopic images show subcellular location of IFITM3-Exos, Δ1–21-Exos, and Δ59–68-Exos in Vero cells. The endolysosomal membranes were stained in green with anti-LAMP-1 antibody, the exosomes were stained in red by Dil dye, and the nuclei were stained in blue with DAPI. Left graph: fluorescence intensity of LAMP-1 (green) and Exos (red) in the regions delineated by a line through ImageJ software. Untreated cells were used as control. (B) Exosomes presenting Δ1–21 or Δ59–68 IFITM3 failed to inhibit ZIKV infection. Vero cells were treated with the exosomes and subsequently inoculated with ZIKV (3×10^5 PFU). ZIKV E protein expression levels of the infected cells were determined by intracellular staining using an anti-E protein antibody and flow cytometry. Mean fluorescence intensity (MFI) of E protein is shown. (C) Exosomes presenting Δ1–21 or Δ59–68 IFITM3 lost the ability to protect cells from ZIKV-induced cell killing. Vero cells were treated with Exos, IFITM3-Exos, Δ1–21- IFITM3-Exos, or Δ59–68-IFITM3-Exos, followed by infection with ZIKV. Cell Counting Kit-8 (CCK-8) assays were used to determine the cell viability. Data are mean ± SEM from triplicate assays. $^*p < 0.05$, $^{**}p < 0.01$.
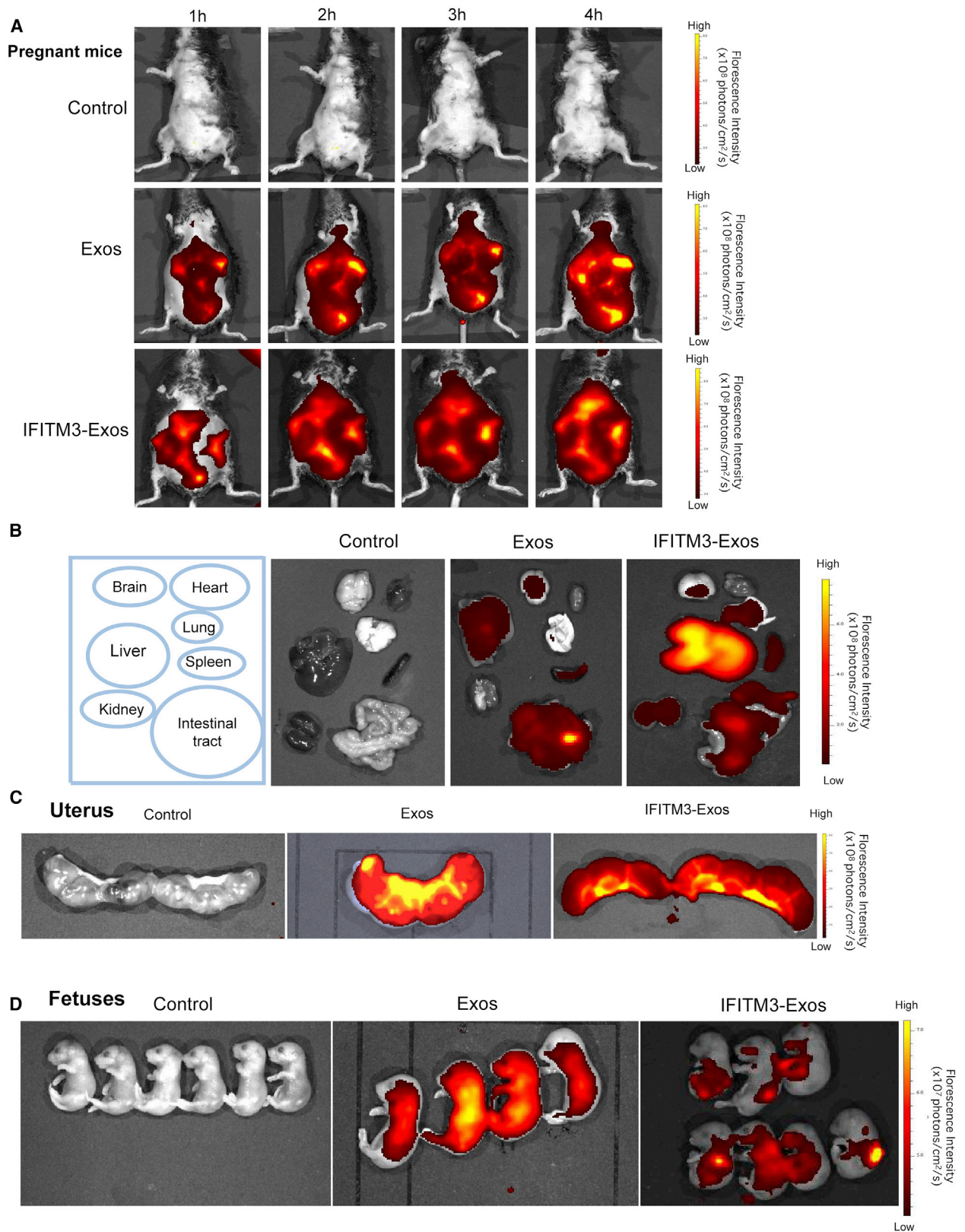
percentage of DiI-positive cells (Figure 5A). Across the range of IFITM3-Exos concentrations tested, BeWo and H295R cells had similar percentages of DiI-positive cells at lower IFITM3-Exos concentrations, while BeWo cells had DiI-positive levels almost twice those of H295R cells (28.59% versus 14.28%, Figure 5A) at higher concentrations.

In order to determine whether the trans-placenta was selective for particle size, we measured the size distribution of the IFITM3-Exos in both the upper and lower chambers using Nanoflow (NanoFCM, China). A BeWo cell monolayer was prepared at the upper chamber in a transwell culture as shown in Figure 5B. IFITM3-Exos were administrated into the upper chamber, incubated with the monolayer from 30 min to 6 h, and the EVs from both upper and lower chambers were analyzed for their size distribution. The sizes of the EVs showed no significant differences in the upper and lower chambers at all time points analyzed (Figure 5B), suggesting that the EV trans-BeWo cell monolayers were not selective in size.

The trans-placental kinetics of IFITM3-Exos were also determined by measuring the amount of IFITM3-Exos in both the upper and lower chambers at various time points using Nanoflow (NanoFCM, China). We found that by 0.5 h, 20% of the IFITM3-Exos were already detectable at the lower chamber and about 60% of the EVs passed the placental BeWo cell monolayer by 1 h, suggesting that the trans-placenta occurred quickly (Figure 5C). The result was consistent with the observation in the mouse model that a significant amount of IFITM3-Exos accumulated at the pregnant mouse's placenta in the first hour of EV administration.

IFITM3-Exos Suppressed ZIKV Infection of Both the Pregnant Mice and the Fetuses

The antiviral activity of the cross-placenta-delivered IFITM3-Exos was investigated *in vivo* by administering IFITM3-Exos or Exos to ZIKV-infected pregnant mice (E13.5) every 2 days through a tail vein injection, at 100 μg of EVs per mouse (Figure 6A), and viral loads were determined in both mothers and fetuses. On day 6 post-infection, the mice were sacrificed and dissected and the viral load in the blood or organs, including spleen, liver, and brain, was determined by qRT-PCR. The results showed that IFITM3-Exos significantly suppressed ZIKV replication in both the pregnant mice and their fetuses. In the pregnant mice, IFITM3-Exos-treated mice had the viral load 2 logs lower than that of the untreated, infected mice, whereas the virus in the fetuses from the IFITM3-Exos-treated mice was almost completely inhibited to the background level of the uninfected mice (Figures 6B and 6C). Similarly, the suppression of ZIKV infection in organs, such as spleen, liver, and brain, was also observed both in the IFITM3-Exos-treated pregnant mice (Figures 6D–6F) and in their fetuses (Figures 6G–6I).

Safety of IFITM3-Exos for Pregnant Mice and Fetuses

Safety is a major consideration for any anti-ZIKV drugs applied to pregnant women and their fetuses. We assessed the safety of IFITM3-Exos in pregnant AG6 mice by examining the potential histopathological changes of the mothers and their fetuses treated with IFITM3-Exos or PBS. As shown in Figure 7A, the hematoxylin-and-eosin-stained sections of livers, kidneys, and spleens from the mice treated with IFITM3-Exos at 1.5 times the therapeutic dose (150 μg/mouse) exhibited no pathological abnormality as compared with those from the mice treated with PBS. None of these tissue sections showed evidence of cell degeneration, necrosis, or infiltration of inflammatory factors. Overall, IFITM3-Exos are safe for both pregnant mice and their fetuses, even at the dose as high as 1.5 times that of the therapeutic dose *in vivo* for ZIKV inhibition. Additionally, serum biochemistry analysis showed that neither creatinine (CRE) nor alanine aminotransferase (ALT) levels increased in animals treated with IFITM3-Exos or control EVs at 1.5 times the therapeutic dose, as compared to those of the mock-treated mice, indicating no significant kidney or liver damage caused by the EV treatment. To further examine the safety of IFITM3-Exos to the placenta and fetuses of pregnant animals, we escalated the dose of IFITM3-Exos to 3 times (to 300 μg/mouse) the therapeutic dose. The hematoxylin-and-eosin-stained sections of placenta from the pregnant mice showed that IFITM3 delivered by IFITM3-Exos did not cause histopathological changes in the placenta, even at 3 times the therapeutic dose (Figure 7D). Moreover, 300 μg/mouse IFITM3-Exos caused no morphological changes to the uteri or the fetuses and no fetal reduction under this condition (Figure 7E).

DISCUSSION

Bioactive proteins have great potential as therapeutics.[30] However, the delivery has limited the use of the proteins for treatment of diseases because of enzymatic degradation and poor penetration of tissues or cells. Particularly for a transmembrane protein, a successful vehicle to deliver it into target cells faces at least two challenges. First, the vehicle must be able to maintain the protein's functional structure to work in cells.[31] Second, during the cross-cell delivery process, it must be able to maintain the protein's structure when going through plasma membrane.[32] As a lipid nanoparticle, EVs can load a transmembrane protein that is derived from the host's membrane and thus maintain the protein's native conformational structure, providing a novel system for effectively delivering bioactive protein as therapeutics.[33] The present study showed that IFITM3 could be effectively delivered by EVs into target cells and tissues and was localized onto the endolysosomal membrane, where IFITM3 works to block virus infection.

IFITM proteins are a family of small transmembrane proteins that are inducible by IFNs. They function as restriction factors to various viral

---

Figure 4. Distribution of Exosomes in Pregnant AG6 Mice

(A) The distribution of the exosomes in a pregnant mouse delivered by tail vein injection was monitored in real time during a 4-h period using an IVIS (Xenogen). Each mouse was injected with 150 μg of DiR-labeled exosomes. (B) Exosome distribution to organs in the mice. (C) Imaging of the uteri from the pregnant mice receiving exosome treatment. (D) Imaging of the fetuses from the uteri of the pregnant mice. Photographs were taken at 4 h after exosome treatment (n = 3).
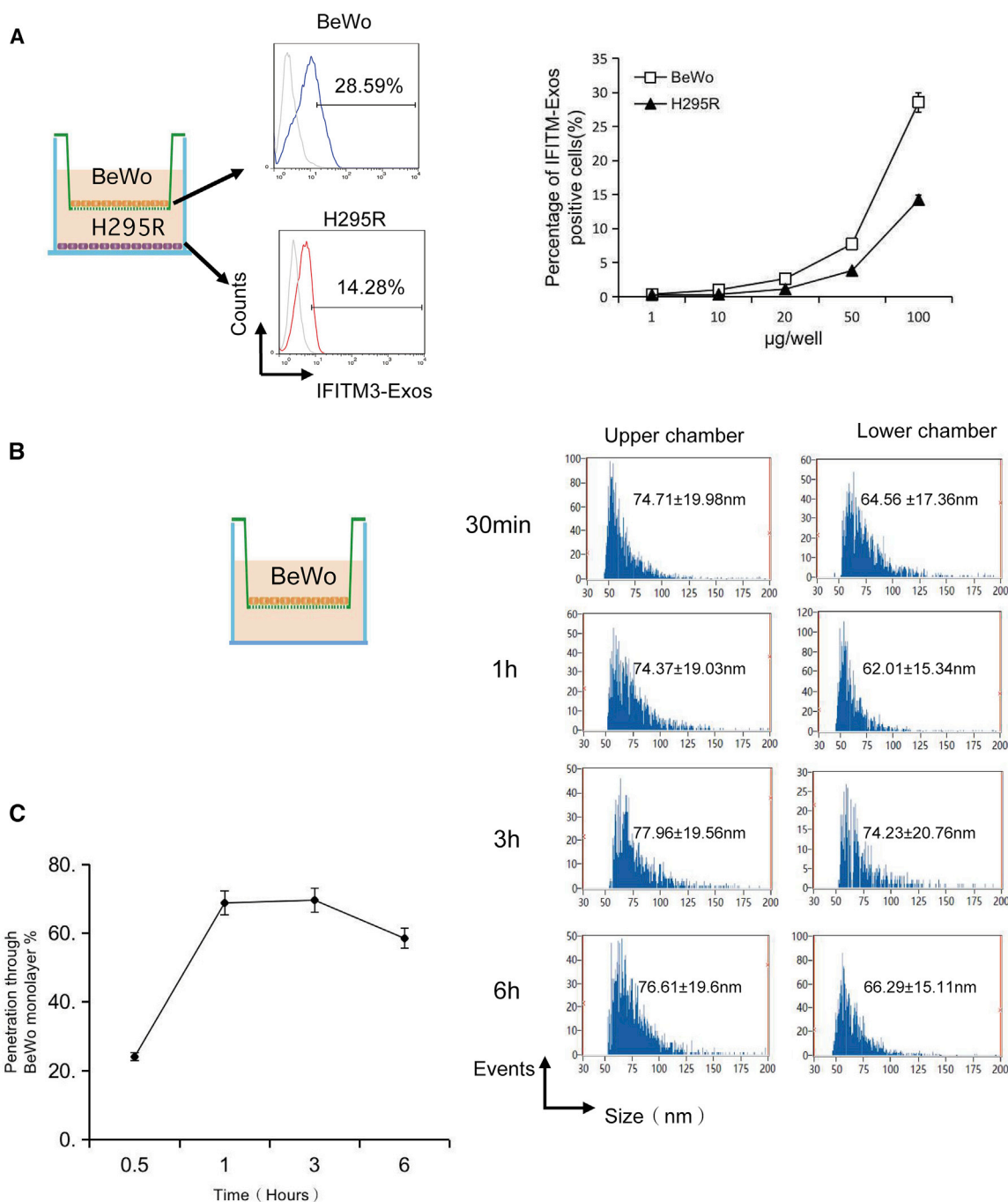
Figure 5. IFITM3-Exos Penetration through the BeWo Cell Monolayer

Schematic illustrations of the transwell assay are shown. A porous (0.4-μm) membrane of the upper chamber allows transfer of exosomes but precludes direct cell-cell contact. A BeWo cell monolayer was formed in the upper chamber, and its integrity was confirmed by trans-epithelial electrical resistance (TEER, e = 140) using a Millicell ESR-2 (Millipore, Bedford, MA, USA). H295R cells were cultured in the lower chamber. Dil-labeled IFITM3-Exos were added to the upper chamber, and the exosome penetration was determined by quantifying exosomes in both the upper and lower chambers. (A) Transwell co-culture of BeWo and H295R cells. Uptake of Dil-labeled IFITM3-Exos by the H295R cells in the lower chamber was compared with that by the BeWo cells in the upper chamber. Binding curves are shown by mean fluorescence intensity in each cell fraction, measured by flow cytometry. (B) Nanoflow (NanoFCM, China) analysis of IFITM3-Exos in the upper and lower chambers for events at 30 min, 1 h, 3 h, and 6 h after the administration of the exosomes into the upper chamber. Numbers are mean ± SEM of the particle sizes measured by three independent experiments. (C) Percentage of the IFITM3-Exos passed through the BeWo cell monolayer at 30 min, 1 h, 3 h, and 6 h measured by Nanoflow (NanoFCM, China) analysis. One-way ANOVA test was performed. Data show the means ± SEMs of three independent experiments.
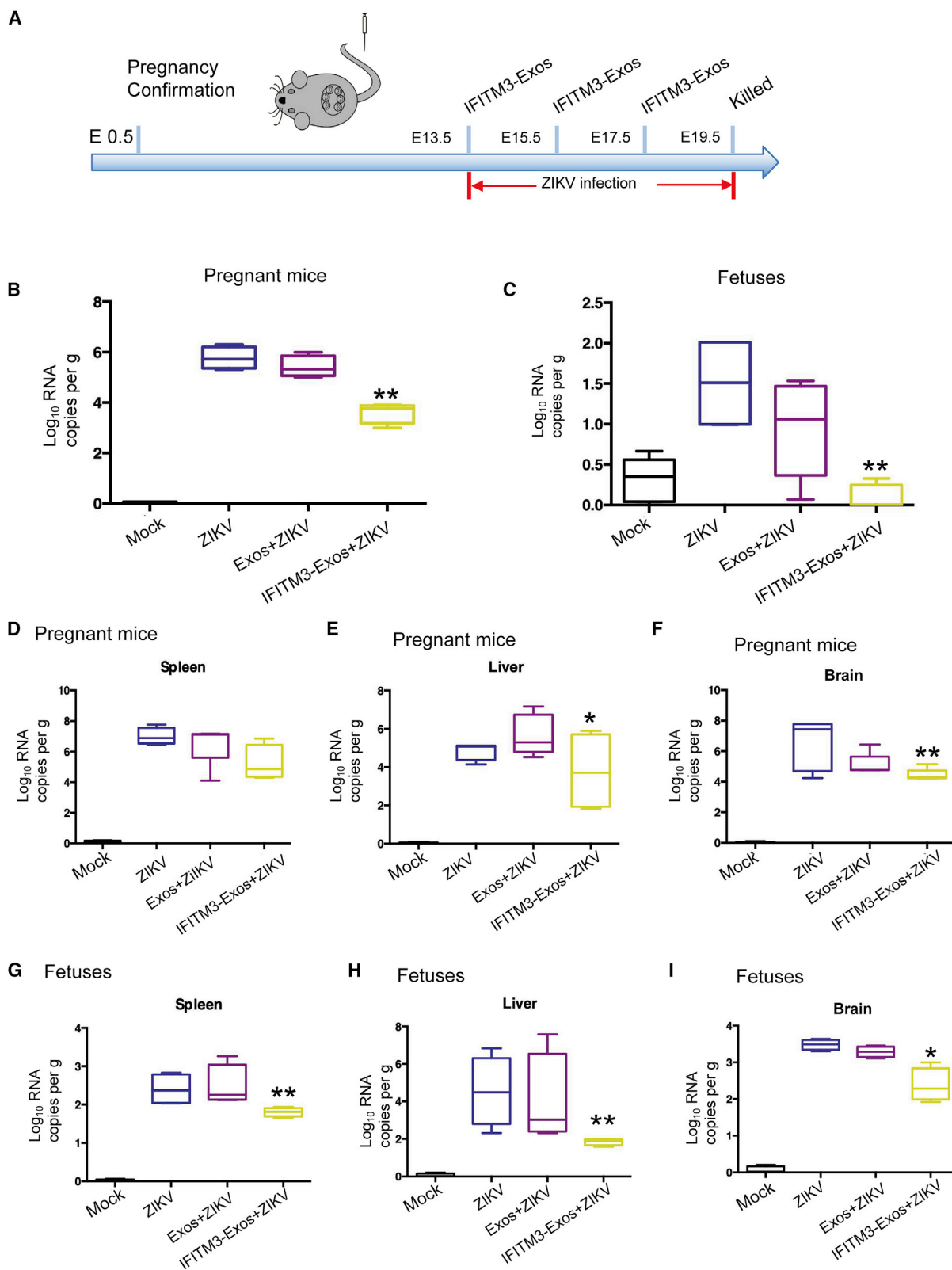
infections by blocking the entry of many enveloped viruses into host cells. Previous studies showed that IFITM1 and IFITM3 played a protective role against ZIKV infection by inhibiting replication of the virus and preventing cell death.[5] To restrict entry, IFITM3 on the surface of lysosomes and late endosomes directly blocks the fusion mediated by the E protein of flavivirus.[24,34] Although a study reported that IFITM3 affected virus-cell binding in vaccinia virus infection,[7] we did not find IFITM3 restriction of ZIKV attachment to the host cells (Figure 2D). Additionally, our results showed that IFITM3-Exos were localized to lysosomes or late endosomes, indicating that the exogenous IFITM3 delivered by EVs was transported to and blocked virus entry via endolysosomes. In contrast, EVs containing IFITM3 mutants could not be effectively delivered to the endolysosomes (Figure 3A). The ZIKV inhibitory activity was demonstrated to be mediated specifically by IFITM3 protein, which was delivered into the target cells by EVs and correctly positioned to endolysosomes, because the EVs containing IFITM3 mutants failed to suppress ZIKV and to protect infected cells from death (Figures 3B and 3C).

Notably, previous studies showed that IFITM3 was upregulated in fetuses[35] and the placenta,[36] suggesting that it may play protective roles during pregnancy in fending off pathogens. Furthermore, the constitutive expression of IFN-stimulated genes (ISGs), including IFITM1 and IFITM3, in the placenta is considered an intrinsic mechanism to protect the developing fetus from viral infection.[12] However, the IFITM levels in the developing fetal organs are low as compared with those in the placenta,[37] providing an opportunity for ZIKV to replicate in the fetuses. Moreover, ZIKV infection can inhibit type I IFN and downstream signaling, thus further suppressing endogenous IFITM expression.[38–40] Therefore, the IFITM3 presented on the surface of EVs is a plausible approach to elevate the IFITM3 in the fetus to combat ZIKV infection, as shown in the current study both in vitro and in vivo. Importantly, exosomal IFITM3 was transported through pregnant mice to their fetuses, concentrated in fetal organs, including brains, and reduced ZIKV loads of both the pregnant mice and the fetuses, demonstrating that EVs can package and effectively transport an exogenous antiviral protein across the placenta to fetuses, and control intrauterine viral infection. Furthermore, IFITM proteins have multiple roles in immune regulation. IFITM3 is also involved in adaptive immunity, regulating CD4+ T helper (Th) differentiation. It is reported to exacerbate Th17-driven inflammation in colitis, and it upregulates c-myc expression to promote tumor proliferation via the extracellular signal-regulated kinase (ERK)1/2 signaling pathway in hepatocellular carcinoma. Taking the multiple regulatory functions of IFITM3 into account, our strategy of utilizing exosomes as a delivery vehicle

provides a novel approach of delivering a complex transmembrane protein into cells in its functional form.

The delivery of IFITM3-containing EVs did not alter the expression of endogenous IFITM3 in the pregnant mouse or in its fetuses at RNA levels (Figures S4A and S4B). We also found that IFITM3-Exos did not cause detectable adverse effects in both the pregnant mice and the fetuses. Importantly, IFITM3-Exos were well tolerated and did not induce a deleterious immune reaction in the pregnant mice or in the fetuses as an autologous protein. Although a recent study revealed that a high level of IFITM expression could inhibit the fusion of trophoblast cells for syncytiotrophoblast formation, the IFITMs did not alter growth of placental trophoblast cells already formed.[41] In the present study, we applied escalating doses to 3 times the therapeutic dose of IFITM3-Exos to determine the safety of IFITM3 to the placenta and the fetuses and did not observe any placental lesions or fetal reduction, demonstrating the in vivo safety of IFITM3-Exos.

The efficiency of cross-placenta delivery of EVs showed that more than 60% of EVs went through the BeWo cell monolayer 1 h after addition. Considering that the EVs crossing the BeWo cell monolayers retained their structural integrity as observed by nano-flow cytometry, we speculated that this penetration occurred through the intercellular space, given that fetal exosomes enter the maternal circulatory system via intercellular space.[42] Additionally, a recent study found that therapeutic exosomal vehicles could readily traverse the extracellular matrix while being transported through tissues.[43] Furthermore, our results from both the BeWo cell model and the animals indicated that some EVs were retained at the placenta, suggesting that part of the EVs entered BeWo cells and others went through intercellular space and reached the fetuses. A previous study using a 3D organ culture model revealed that the placenta was a likely key site of vertical transmission of ZIKV.[44] Therefore, the concentration of IFITM3-Exos at the site of the placenta would contribute to the suppression of fetal infection. However, we did not determine whether the reduction of virus in the fetuses was caused by direct inhibition by IFITM3-Exos, the inhibition of virus in the mother, or both. The control of intrauterine infection of ZIKV is likely a consequence of multiple causes and, nevertheless, the effectiveness of IFITM3-Exos in suppressing viral load in fetuses will be helpful to protect fetuses from the virus-induced damage.

Notably, we observed significant suppression of ZIKV infection in the fetal brain by IFITM3-Exos. Considering that viral load of ZIKV in the infected fetuses predicted the occurrence of neutral nerve system deformities,[45] our results suggest that IFITM3-Exos could be a

Figure 6. The Antiviral Activity of IFITM3-Exos

Pregnant mice were infected by ZIKV by a subcutaneous route in the footpad at 10^3 PFU per mouse for 6 days and treated with IFITM3-Exos or Exos (control) three times (100 μg per mouse) as indicated. At day 6 post-infection, sera were collected by retro-orbital bleeding for viremia detection. (A) Schematic illustration. (B) Viremia of the pregnant AG6 mice. (C) Viremia of the fetuses (the labels for the y axis have differing sizes in B and C). The viral RNA load in each serum sample was determined by qRT-PCR. (D–F) Viral RNA load in spleen (D), liver (E), and brain (F) of the pregnant AG6 mice. (G–I) Viral RNA load in spleen (D), liver (E), and brain (F) of the fetuses. The organs were collected by dissection, and qRT-PCR was performed to determine the viral RNA load. All bars reflect median values. *p < 0.05, **p < 0.01, by Mann-Whitney test (n = 5–6).
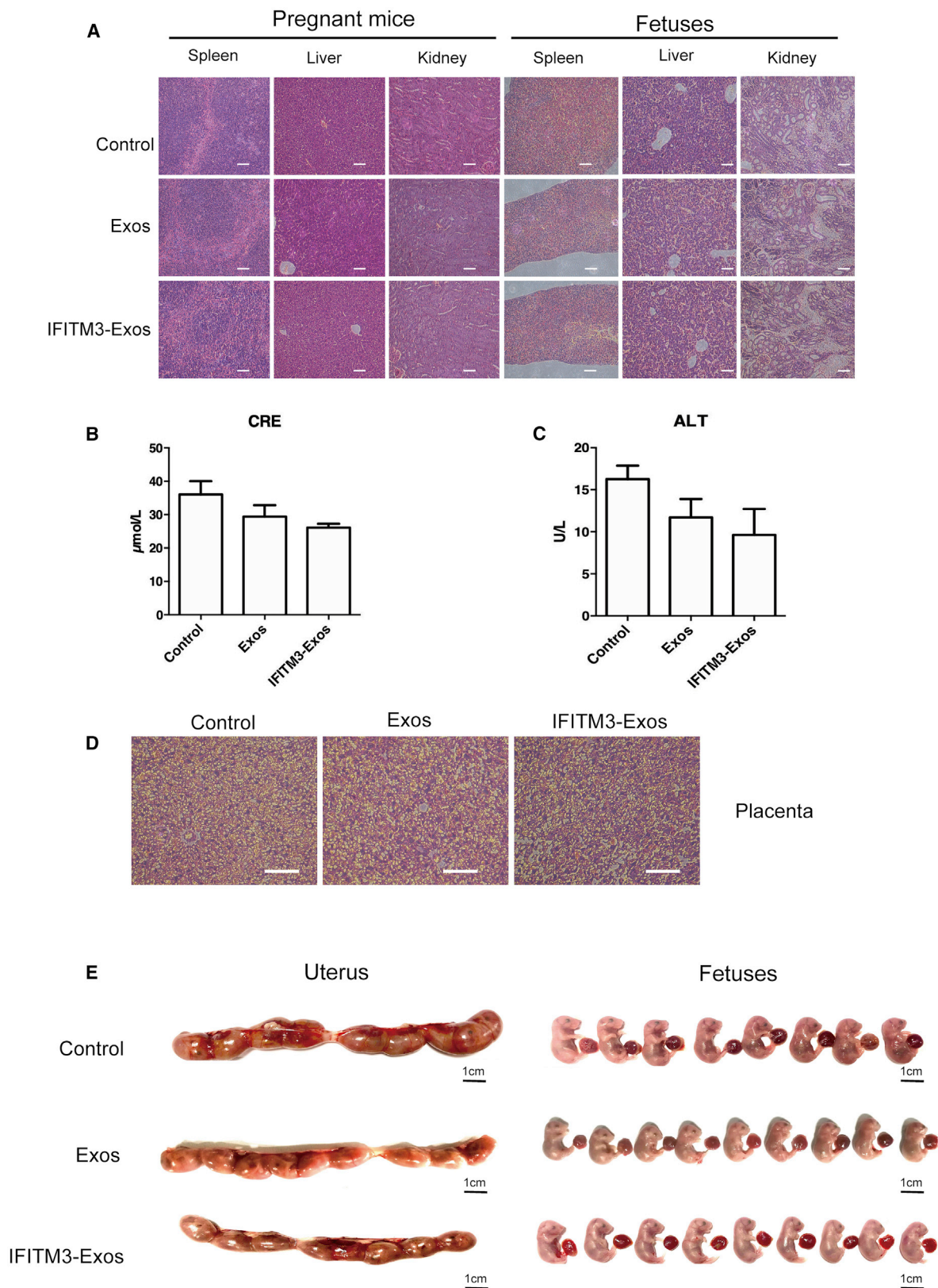
(legend on next page)

potential therapy for the treatment of ZIKV infection in pregnant mothers and prevent virus-induced CNS deformities. While application of IFNs has been highly appreciated in clinical practice, problems associated with the use of IFNs, such as suboptimal efficacy against many viruses and varied degrees of adverse effects caused by IFN treatment, remain unsolved.[46] In the intensive efforts of identifying and developing new endogenous anti-viral factors with potential clinical applicability, ISGs such as IFITM molecules have been attractive candidate agents for therapeutic purposes. However, methods to elevate the IFITM3 expression in fetuses are limited. Gene modulation cannot be applied to fetuses out of safety concerns. In such a context, exosomal IFITM3, as reported by the present study, appears to represent a novel, attractive anti-viral strategy, as our specially engineered EVs can serve as nano-vehicles for the delivery of complex transmembrane proteins. Generally in our model systems, 293T cell-derived EVs were well tolerated and safe *in vivo*. Nevertheless, the present study demonstrated in principle the feasibility of using EVs to deliver an exogenous bioactive transmembrane protein across the placenta to the fetus to control intrauterine viral infection.

MATERIALS AND METHODS

Cell Culture and Virus

293T and HeLa cells were maintained in Dulbecco's modified Eagle's medium (DMEM; Invitrogen, Carlsbad, CA, USA) supplemented with 10% fetal bovine serum (FBS; HyClone, Logan, UT, USA), 2 mM L-glutamine, 100 μg/mL streptomycin, and 100 U/mL penicillin (Invitrogen). HA-IFITM3 plasmid was a gift from Howard Hang & Jacob Yount (Addgene plasmid).[47] HA-IFITM3Δ1–21 and HA-IFITM3Δ59–68 plasmids were from GenScript Biotech (Nanjing, China). H295R and BeWo cells were cultured in DMEM/nutrient mixture F12 (DMEM/F12) without phenol red containing 1.2 g/L sodium bicarbonate and 2 mg/L pyridoxine HCl (Gibco, Lucerne, Switzerland). The medium was completed with 2.5% NuSerum (VWR International, Radnor, PA, USA) and 1% penicillin/streptomycin (Gibco). 293T cells were transfected with the vector expressing the IFITM3 using polyethylenimine (PEI) transfection reagent (Invitrogen, USA). The cultures were maintained at 37°C in a humidified atmosphere of 5% CO_2. ZIKV (SZ01) strain was kindly provided by Prof. Xia Jin (Institut Pasteur of Shanghai, Chinese Academy of Sciences [CAS]) and was propagated in the C6/36 cell line. ZIKV strain SZ01/2016 (GenBank: KU866423) was isolated from a patient who returned from Samoa.[48]

Isolation of EVs

Prior to cell culture, DMEM containing 20% FBS was centrifuged at 120,000 × g for 2 h to deplete serum exosomes. 293T cells, used for exosome production, were cultured in 30 mL of DMEM + 5% exosome-depleted FBS in a 150-mm dish and maintained in 5% CO_2 at 37°C for 48 h. Exosomes were isolated from the 30-mL harvested supernatant according to a previous report.[49] The filtrate was centrifuged at 110,000 × g for 120 min at 4°C in a type Ti70 rotor, using an L-80XP ultracentrifuge (Beckman Coulter, Brea, CA, USA, USA). The exosome pellet was resuspended in PBS and ultracentrifuged again at 110,000 × g for 120 min. The pelleted exosomes were resuspended in PBS and analyzed using a Micro BCA (bicinchoninic acid) protein assay kit (Pierce, Rockford, IL, USA) or by western blot analysis of exosomal markers using antibodies specific for ALIX, Flotillin 1, GM130, and HA-tag (Proteintech, Wuhan, China).

Characterization of EVs by NTA

NTA was performed with a NanoSight LM10-HSB instrument (A&P Instrument, UK) using EVs (10 ng/mL, protein equivalent) purified from 100 mL of 293T cell culture supernatant. The median size and size distribution were captured and analyzed with the NTA 2.2 Analytical Software suite. All procedures were performed at room temperature.

Co-culture of EVs and Cells

To investigate the uptake of IFITM3-Exos by H295R cells, the cells were incubated with 10 mM DiI-labeled IFITM3-Exos at 37°C for 30 min. Co-culture setup was as previously described,[29,49] except for the replacement of 24-well culture plates with 6-well plates. For hormone quantification and RNA extraction under co-culture conditions, 7.5 × 10^5 H295R cells were seeded in 2 mL per well in six-well plates, and 3.5 × 10^5 BeWo cells were seeded in 1.5 mL in transwell inserts (polycarbonate membrane with 0.4-μm pores, Corning Life Sciences, Corning, NY, USA). Importantly, both batches of cells were exposed to treated co-culture medium. All experiments were performed using cells with passage numbers between 8 and 25. Exposures to IFITM3-Exos were for 30 min, 1 h, 3 h, and 6 h in an incubator at 37°C with a humidified atmosphere containing 5% CO_2.

Flow Cytometry

For fluorescence-activated cell sorting (FACS), exosomes from 293T cells were adsorbed onto 4-μm aldehyde-sulfate latex beads (Interfacial Dynamics, Tualatin, OR, USA), incubated with Alexa Fluor phycoerythrin (PE)-conjugated anti-HA-tag antibody, Alexa Fluor allophycocyanin (APC)-conjugated anti-CD81 antibody (all purchased from BD Pharmingen, San Jose, CA, USA), and analyzed on a FACSCalibur system (Becton Dickinson, San Diego, CA, USA). Part of the exosomes were also directly analyzed by Nanoflow

---

Figure 7. Safety Analysis of IFITM3-Exos for Pregnant Mice and Fetuses

(A) Hematoxylin and eosin staining of tissues, including livers, kidneys, and spleens from the pregnant mice and their fetuses of various treatment groups. Scale bars, 100 μm. (B and C) Serum creatinine (CRE) level (B) and alanine aminotransferase (ALT) level (C) of the pregnant mice were measured by ALT and CRE assay kits, respectively. The assays were performed before the first injection and 6 days after the third injection of IFITM3-Exos or Exos (100 μg per mouse). Data are mean ± SEM of three independent experiments. (D) Hematoxylin and eosin staining of placental tissue sections from an untreated pregnant mouse (control) and mice treated with an escalating dose of Exos or IFITM3-Exos (300 μg per mouse) for 6 days. (E) Photographs of the uterus and the fetuses from an untreated pregnant mouse (control) and mice treated with Exos or IFITM3-Exos for 6 days (n = 3–5).

(NanoFCM, Xiamen, China), according to the manufacturer's directions.

Western Blot
For western blot analysis, ultracentrifuged exosomal pellets were lysed with radioimmunoprecipitation assay buffer (RIPA) buffer (Cell Signaling Technology) containing a protease inhibitor cocktail (Calbiochem). The total protein was determined by using a BCA kit, and an equivalent amount (25 μg) of exosomal protein was resolved by SDS-PAGE and transferred to nitrocellulose membranes. The blots were probed overnight at 4°C with antibodies specific for ALIX, Flotillin 1, and GM130. IRDye immunoglobulin G (IgG) was used as secondary antibody (1:10,000) for 30 min. Bands were visualized on a LI-COR Odyssey infrared imager (LI-COR Biosciences).

Vero Cell Plaque Assay
Cells were plated at 1×10^5 cells/well in a 24-well culture plate and incubated overnight at 37°C, 5% CO_2. At day 2, the cells were washed with warm DMEM before virus infection. For a part of samples, Vero cells were incubated with 60 μg/well of Exos or IFITM3-Exos. ZIKV samples were diluted to 1×10^3 PFU in DMEM supplemented with 1% penicillin/streptomycin (P/S) and then incubated with Vero cells for 2 h for virus adsorption. The viral inoculum was removed and DMEM was supplemented with 1.5% FBS, 1% P/S, and 1% carboxymethyl cellulose (CMC). Vero cells were incubated with the CMC overlay for 5 days, and then the overlay was removed. Cells were fixed with 4% paraformaldehyde for 4 h, then stained with 2.5% crystal violet solution for plaque counting.

In Vivo Imaging
Mice were anesthetized via isoflurane inhalation, and intraperitoneally injected with 150 μg of DiR-labeled exosomes. Bioluminescence imaging was performed 10 min after injection with an IVIS (Xenogen). The section of interest was defined manually, and bioluminescence was expressed as photon flux values (photons/s/cm^2/steradian). To determine the distribution of IFITM3-Exos in organs, all pregnant mice were sacrificed and the dissected brains, livers, kidneys, spleens, lungs, hearts, intestinal tracts, uteri, and fetuses were imaged and the average radiant efficiency was calculated. The fetuses in the uteri of two groups were applied to paraformaldehyde (PFA)-fixed paraffin sections to illustrate the distribution of IFITM3-Exos in the placenta and fetuses.

Virus Binding and Entry Assays
The binding and entry experiments were performed as described previously.[6,50] Briefly, for virus binding experiments, cells were seeded in 12-well plates and cultured for 24 h, followed by inoculation with ZIKV at 3×10^5 PFU on ice for 1 h to allow virus binding but impeding cell entry. Unbound virus was removed and the cells were harvested to determine the amount of viral RNA accumulation by qRT-PCR. To assess ZIKV entry into cells via endocytosis, after binding on ice for 1 h, virus inocula were removed after 1 h of binding on ice, and the infected cells were washed with PBS followed by incubation with pre-warmed DMEM for 10 min at 37°C to initiate virus cell entry. For assessments of post-entry infection steps, after virus binding and

entry procedures were finished, HeLa cells were subsequently treated with IFITM3-Exos or Exos. Total cellular RNA was extracted to measure relative viral RNA that had entered cells by qRT-PCR.

Antiviral Efficacy of IFITM3-Exos in AG6 Mice
Six-week-old sex-matched AG6 mice were assigned randomly to two groups (n = 5) and infected with 10^3 PFU of ZIKV (SZ01) via a subcutaneous route in the footpad. Then, the infected mice were intravenously (i.v.) administered IFITM3-Exos at 100 μg of IFITM3-Exos or Exos every other day for a total of four injections. The examination of AG6 mice was carried out as previously described.[51]

Safety of IFITM3-Exos for Pregnant AG6 Mice and Fetuses
AG6 mice (E13.5–E19.5, n = 5) were assigned randomly into three groups and injected i.v. with IFITM3-Exos, Exos at 150 or 300 μg, or PBS as control every other day for 6 days. Serum ALT and CRE levels in the sera collected from the tails were measured by using ALT and CRE assay kits (Jiangcheng Bio, Nanjing, China) after 6 days, respectively. The pregnant mice and their fetuses in each group were sacrificed and the livers, kidneys, and spleens were collected for hematoxylin and eosin staining. All animal studies were carried out according to the ethical guidelines and approval by the Institutional Laboratory Animal Care and Use Committee at Nanjing University.

Statistical Analysis
All *in vitro* experiments were performed at least three times. The results are described as mean ± SEM. Statistical analysis was performed by one-way analysis of variance (ANOVA), and comparisons among groups were performed by a Tukey's honestly significant difference test or t test.

SUPPLEMENTAL INFORMATION
Supplemental Information can be found online at https://doi.org/10.1016/j.ymthe.2020.09.026.

AUTHOR CONTRIBUTIONS
X.Z., M.Y., and T.Z. conducted the experiments; X.Z. and N.Z. analyzed the data; and Z.W., N.Z., and X.Z. designed the study and wrote the manuscript.

CONFLICTS OF INTEREST
The authors declare no competing interests.

REFERENCES
1. Heukelbach, J., Alencar, C.H., Kelvin, A.A., de Oliveira, W.K., and Pamplona de Góes Cavalcanti, L. (2016). Zika virus outbreak in Brazil. J. Infect. Dev. Ctries. *10*, 116–120.

2. Watanabe, S., Tan, N.W.W., Chan, K.W.K., and Vasudevan, S.G. (2019). Assessing the utility of antivirals for preventing maternal-fetal transmission of Zika virus in pregnant mice. Antiviral Res. *167*, 104–109.

3. Best, K., Guedj, J., Madelain, V., de Lamballerie, X., Lim, S.Y., Osuna, C.E., Whitney, J.B., and Perelson, A.S. (2017). Zika plasma viral dynamics in nonhuman primates provides insights into early infection and antiviral strategies. Proc. Natl. Acad. Sci. USA *114*, 8847–8852.

4. Chandy, B.K. (2012). WHO-Facts Sheet. Kuwait Med. J. *44*, 362–367.

5. Brass, A.L., Huang, I.C., Benita, Y., John, S.P., Krishnan, M.N., Feeley, E.M., Ryan, B.J., Weyer, J.L., van der Weyden, L., Fikrig, E., et al. (2009). The IFITM proteins mediate cellular resistance to influenza A H1N1 virus, West Nile virus, and dengue virus. Cell *139*, 1243–1254.

6. Weidner, J.M., Jiang, D., Pan, X.B., Chang, J., Block, T.M., and Guo, J.T. (2010). Interferon-induced cell membrane proteins, IFITM3 and tetherin, inhibit vesicular stomatitis virus infection via distinct mechanisms. J. Virol. *84*, 12646–12657.

7. Li, C., Du, S., Tian, M., Wang, Y., Bai, J., Tan, P., Liu, W., Yin, R., Wang, M., Jiang, Y., et al. (2018). The host restriction factor interferon-inducible transmembrane protein 3 inhibits vaccinia virus infection. Front. Immunol. *9*, 228.

8. Chesarino, N.M., McMichael, T.M., and Yount, J.S. (2014). Regulation of the trafficking and antiviral activity of IFITM3 by post-translational modifications. Future Microbiol. *9*, 1151–1163.

9. Savidis, G., Perreira, J.M., Portmann, J.M., Meraner, P., Guo, Z., Green, S., and Brass, A.L. (2016). The IFITMs inhibit Zika virus replication. Cell Rep. *15*, 2323–2330.

10. Monel, B., Compton, A.A., Bruel, T., Amraoui, S., Burlaud-Gaillard, J., Roy, N., Guivel-Benhassine, F., Porrot, F., Génin, P., Meertens, L., et al. (2017). Zika virus induces massive cytoplasmic vacuolization and paraptosis-like death in infected cells. EMBO J. *36*, 1653–1668.

11. Diamond, M.S., and Farzan, M. (2013). The broad-spectrum antiviral functions of IFIT and IFITM proteins. Nat. Rev. Immunol. *13*, 46–57.

12. Yockey, L.J., and Iwasaki, A. (2018). Interferons and proinflammatory cytokines in pregnancy and fetal development. Immunity *49*, 397–412.

13. Familtseva, A., Jeremic, N., and Tyagi, S.C. (2019). Exosomes: cell-created drug delivery systems. Mol. Cell. Biochem. *459*, 1–6.

14. McGough, I.J., and Vincent, J.P. (2016). Exosomes in developmental signalling. Development *143*, 2482–2493.

15. Zou, X., Yuan, M., Zhang, T., Wei, H., Xu, S., Jiang, N., Zheng, N., and Wu, Z. (2019). Extracellular vesicles expressing a single-chain variable fragment of an HIV-1 specific antibody selectively target Env[+] tissues. Theranostics *9*, 5657–5671.

16. Zhang, M., Zang, X., Wang, M., Li, Z., Qiao, M., Hu, H., and Chen, D. (2019). Exosome-based nanocarriers as bio-inspired and versatile vehicles for drug delivery: recent advances and challenges. J. Mater. Chem. B Mater. Biol. Med. *7*, 2421–2433.

17. O'Brien, K., Breyne, K., Ughetto, S., Laurent, L.C., and Breakefield, X.O. (2020). RNA delivery by extracellular vesicles in mammalian cells and its applications. Nat. Rev. Mol. Cell Biol. *21*, 585–606.

18. Zhu, X., He, Z., Yuan, J., Wen, W., Huang, X., Hu, Y., Lin, C., Pan, J., Li, R., Deng, H., et al. (2015). IFITM3-containing exosome as a novel mediator for anti-viral response in dengue virus infection. Cell. Microbiol. *17*, 105–118.

19. Sheller-Miller, S., Trivedi, J., Yellon, S.M., and Menon, R. (2019). Exosomes cause preterm birth in mice: evidence for paracrine signaling in pregnancy. Sci. Rep. *9*, 608.

20. Stenqvist, A.C., Nagaeva, O., Baranov, V., and Mincheva-Nilsson, L. (2013). Exosomes secreted by human placenta carry functional Fas ligand and TRAIL molecules and convey apoptosis in activated immune cells, suggesting exosome-mediated immune privilege of the fetus. J. Immunol. *191*, 5515–5523.

21. Sarker, S., Scholz-Romero, K., Perez, A., Illanes, S.E., Mitchell, M.D., Rice, G.E., and Salomon, C. (2014). Placenta-derived exosomes continuously increase in maternal circulation over the first trimester of pregnancy. J. Transl. Med. *12*, 204.

22. Jia, R., Xu, F., Qian, J., Yao, Y., Miao, C., Zheng, Y.M., Liu, S.L., Guo, F., Geng, Y., Qiao, W., and Liang, C. (2014). Identification of an endocytic signal essential for the antiviral action of IFITM3. Cell. Microbiol. *16*, 1080–1093.

23. Compton, A.A., Roy, N., Porrot, F., Billet, A., Casartelli, N., Yount, J.S., Liang, C., and Schwartz, O. (2016). Natural mutations in IFITM3 modulate post-translational regulation and toggle antiviral specificity. EMBO Rep. *17*, 1657–1671.

24. Chesarino, N.M., Compton, A.A., McMichael, T.M., Kenney, A.D., Zhang, L., Soewarna, V., Davis, M., Schwartz, O., and Yount, J.S. (2017). IFITM3 requires an amphipathic helix for antiviral activity. EMBO Rep. *18*, 1740–1751.

25. Coyne, C.B., and Lazear, H.M. (2016). Zika virus—reigniting the TORCH. Nat. Rev. Microbiol. *14*, 707–715.

26. Walker, C.L., Little, M.E., Roby, J.A., Armistead, B., Gale, M., Jr., Rajagopal, L., Nelson, B.R., Ehinger, N., Mason, B., Nayeri, U., et al. (2019). Zika virus and the non-microcephalic fetus: why we should still worry. Am. J. Obstet. Gynecol. *220*, 45–56.

27. Yong, T., Zhang, X., Bie, N., Zhang, H., Zhang, X., Li, F., Hakeem, A., Hu, J., Gan, L., Santos, H.A., and Yang, X. (2019). Tumor exosome-based nanoparticles are efficient drug carriers for chemotherapy. Nat. Commun. *10*, 3838.

28. Gazdar, A.F., Oie, H.K., Shackleton, C.H., Chen, T.R., Triche, T.J., Myers, C.E., Chrousos, G.P., Brennan, M.F., Stein, C.A., and La Rocca, R.V. (1990). Establishment and characterization of a human adrenocortical carcinoma cell line that expresses multiple pathways of steroid biosynthesis. Cancer Res. *50*, 5488–5496.

29. Hudon Thibeault, A.A., Deroy, K., Vaillancourt, C., and Sanderson, J.T. (2014). A unique co-culture model for fundamental and applied studies of human fetoplacental steroidogenesis and interference by environmental chemicals. Environ. Health Perspect. *122*, 371–377.

30. Leader, B., Baca, Q.J., and Golan, D.E. (2008). Protein therapeutics: a summary and pharmacological classification. Nat. Rev. Drug Discov. *7*, 21–39.

31. Pisal, D.S., Kosloski, M.P., and Balu-Iyer, S.V. (2010). Delivery of therapeutic proteins. J. Pharm. Sci. *99*, 2557–2575.

32. Sharma, A.R., Kundu, S.K., Nam, J.S., Sharma, G., Priya Doss, C.G., Lee, S.S., and Chakraborty, C. (2014). Next generation delivery system for proteins and genes of therapeutic purpose: why and how? BioMed Res. Int. *2014*, 327950.

33. Swaminathan, J., and Ehrhardt, C. (2012). Liposomal delivery of proteins and peptides. Expert Opin. Drug Deliv. *9*, 1489–1503.

34. Feeley, E.M., Sims, J.S., John, S.P., Chin, C.R., Pertel, T., Chen, L.M., Gaiha, G.D., Ryan, B.J., Donis, R.O., Elledge, S.J., and Brass, A.L. (2011). IFITM3 inhibits influenza A virus infection by preventing cytosolic entry. PLoS Pathog. *7*, e1002337.

35. Wu, X., Dao Thi, V.L., Huang, Y., Billerbeck, E., Saha, D., Hoffmann, H.H., Wang, Y., Silva, L.A.V., Sarbanes, S., Sun, T., et al. (2018). Intrinsic immunity shapes viral resistance of stem cells. Cell *172*, 423–438.e25.

36. Klein, C., Bauersachs, S., Ulbrich, S.E., Einspanier, R., Meyer, H.H., Schmidt, S.E., Reichenbach, H.D., Vermehren, M., Sinowatz, F., Blum, H., and Wolf, E. (2006). Monozygotic twin model reveals novel embryo-induced transcriptome changes of bovine endometrium in the preattachment period. Biol. Reprod. *74*, 253–264.

37. Mikedis, M.M., and Downs, K.M. (2013). Widespread but tissue-specific patterns of interferon-induced transmembrane protein 3 (IFITM3, FRAGILIS, MIL-1) in the mouse gastrula. Gene Expr. Patterns *13*, 225–239.

38. Grant, A., Ponia, S.S., Tripathi, S., Balasubramaniam, V., Miorin, L., Sourisseau, M., Schwarz, M.C., Sánchez-Seco, M.P., Evans, M.J., Best, S.M., and García-Sastre, A. (2016). Zika virus targets human STAT2 to inhibit type I interferon signaling. Cell Host Microbe *19*, 882–890.

39. Kumar, A., Hou, S., Airo, A.M., Limonta, D., Mancinelli, V., Branton, W., Power, C., and Hobman, T.C. (2016). Zika virus inhibits type-I interferon production and downstream signaling. EMBO Rep. *17*, 1766–1775.

40. Ngueyen, T.T.N., Kim, S.J., Lee, J.Y., and Myoung, J. (2019). Zika virus proteins NS2A and NS4A are major antagonists that reduce IFN-β promoter activity induced by the MDA5/RIG-I signaling pathway. J. Microbiol. Biotechnol. *29*, 1665–1674.

41. Buchrieser, J., Degrelle, S.A., Couderc, T., Nevers, Q., Disson, O., Manet, C., Donahue, D.A., Porrot, F., Hillion, K.H., Perthame, E., et al. (2019). IFITM proteins inhibit placental syncytiotrophoblast formation and promote fetal demise. Science *365*, 176–180.

42. Sheller-Miller, S., Choi, K., Choi, C., and Menon, R. (2019). Cyclic-recombinase-reporter mouse model to determine exosome communication and function during pregnancy. Am. J. Obstet. Gynecol. *221*, 502.e1–502.e12.

43. Lenzini, S., Bargi, R., Chung, G., and Shin, J.W. (2020). Matrix mechanics and water permeation regulate extracellular vesicle transport. Nat. Nanotechnol. *15*, 217–223.

44. Weisblum, Y., Oiknine-Djian, E., Vorontsov, O.M., Haimov-Kochman, R., Zakay-Rones, Z., Meir, K., Shveiky, D., Elgavish, S., Nevo, Y., Roseman, M., et al. (2017). Zika virus infects early- and midgestation human maternal decidual tissues, inducing distinct innate tissue responses in the maternal-fetal interface. J. Virol. *91*, e01905-16.

45. Chimelli, L., and Avvad-Portari, E. (2018). Congenital Zika virus infection: a neuropathological review. Childs Nerv. Syst. *34*, 95–99.

46. Cid, M.C., Robert, J., Trejo, O., Hernandez, J., delRio, A., Grau, J.M., et al. (1997). Treatment with interferon alpha (IFN alpha) may worsen cryoglobulinemia-related ischemic lesions: An adverse effect potentially related to its anti-angiogenic activity. Arthritis Rheum. *40*, 229.

47. Yount, J.S., Moltedo, B., Yang, Y.Y., Charron, G., Moran, T.M., López, C.B., and Hang, H.C. (2010). Palmitoylome profiling reveals S-palmitoylation-dependent antiviral activity of IFITM3. Nat. Chem. Biol. *6*, 610–614.

48. Deng, Y.Q., Zhao, H., Li, X.F., Zhang, N.N., Liu, Z.Y., Jiang, T., Gu, D.Y., Shi, L., He, J.A., Wang, H.J., et al. (2016). Isolation, identification and genomic characterization of the Asian lineage Zika virus imported to China. Sci. China Life Sci. *59*, 428–430.

49. Yang, Y., Hong, Y., Nam, G.H., Chung, J.H., Koh, E., and Kim, I.S. (2017). Virus-mimetic fusogenic exosomes for direct delivery of integral membrane proteins to target cell membranes. Adv. Mater. *29*, 1605604.

50. Kanlaya, R., Pattanakitsakul, S.N., Sinchaikul, S., Chen, S.T., and Thongboonkerd, V. (2010). Vimentin interacts with heterogeneous nuclear ribonucleoproteins and dengue nonstructural protein 1 and is important for viral replication and release. Mol. Biosyst. *6*, 795–806.

51. Yu, Y., Deng, Y.Q., Zou, P., Wang, Q., Dai, Y., Yu, F., Du, L., Zhang, N.N., Tian, M., Hao, J.N., et al. (2017). A peptide-based viral inactivator inhibits Zika virus infection in pregnant mice and fetuses. Nat. Commun. *8*, 15672.